Available online at www.sciencedirect.com
SCIENCE DIRECT®
Journal of Sound and Vibration 290 (2006) 555–571
JOURNAL OF SOUND AND VIBRATION
www.elsevier.com/locate/jsvi

Frequency-domain subspace identification using FRF data from arbitrary signals

B. Cauberghe*, P. Guillaume, R. Pintelon, P. Verboven

Vrije Universiteit Brussel, TW-WERK, Plein Laan 2, B-1050 Brussel, Belgium

Received 28 August 2003; received in revised form 10 January 2005; accepted 1 April 2005
Available online 15 December 2005

Abstract

Recently an extension of the frequency-domain subspace identification methods was developed that can cope with arbitrary excitation signals and transient effects. In this paper the implications of this extended model are investigated for the H_1 estimator. It is shown that an extended model makes it possible to start from frequency response functions (FRFs) without suffering from leakage, by modelling the initial conditions of each data block used in the averaging procedure of the H_1 estimator. In this way the measurements can be averaged in order to reduce both the data set and the noise levels without introducing bias errors caused by leakage phenomena. It is shown by both simulations and real-life measurements that the presented approach improves the modal parameter estimates and in particular the damping estimates.
© 2005 Published by Elsevier Ltd.

1. Introduction

Frequency-domain system identification generally assumes that the input and output signals are periodic or time limited within the observation time. This is necessary to guarantee leakage-free spectra calculated through the discrete Fourier transform. Often in practice a window, e.g. Hanning window, is used to reduce errors introduced by leakage phenomena, although it is known that for short data sequences these windows introduce bias errors in the final estimated parameters and in particular in the damping values.

*Corresponding author. Tel.: +32 2 629 2805; fax: +32 2 629 2865.
E-mail address: bart.cauberghe@vub.ac.be (B. Cauberghe).

0022-460X/$ - see front matter © 2005 Published by Elsevier Ltd.
doi:10.1016/j.jsv.2005.04.021

In Ref. [1] it is shown for single input/single output (SISO) systems that by using an additional 'transient' polynomial in a rational fraction polynomial model, the 'transient' polynomial takes into account the initial and final conditions of the experiment and the bias error due to leakage is eliminated.

A generalization for multiple input/multiple output (MIMO) systems modelled by a common denominator model is used in Refs. [2,3] to process short data sequences. In these references the least-squares complex frequency (LSCF) domain modal parameter estimation method is generalized to take into account the initial and final conditions. In Refs. [4,5] this idea is applied for state-space frequency-domain models. In this present paper, that key idea is applied for frequency-domain MIMO state-space models starting from frequency response function (FRF) data. The frequency-domain subspace identification method in this paper is based on Refs. [6,7] which is a frequency-domain counterpart of the deterministic time-domain subspace approach [8].

In Section 2 of this paper it will be briefly shown that the discrete Fourier spectra of the input and output signals satisfy an extended state-space model that includes the initial and final conditions of each state. In Section 3, this extended state-space model is further developed for the identification starting from FRF data obtained by an H_1 estimator [9]. Section 4 gives a brief introduction and an overview of the subspace identification algorithm used for the identification of the model, while Section 5 contains some general remarks. In Section 6, the theoretical results are verified by means of simulations and the applicability of the method to solve complex modelling problems is illustrated by means of a modal analysis experiment performed on a subframe of a car.

2. State-space model for arbitrary signals

Consider a linear time-invariant state-space model. Assume that the input and output samples are exactly known in the time interval $[0,(N-1)T_s]$ and unknown outside this time interval. The discrete input $u_n \in \mathbf{R}^{N_i \times 1}$ and output $y_n \in \mathbf{R}^{N_o \times 1}$ samples satisfy the following difference equation:

$$x_{n+1} = Ax_n + Bu_n, \tag{1}$$

$$y_n = Cx_n + Du_n \tag{2}$$

with $x_n \in \mathbf{R}^{N_s \times 1}$ (N_s the number of states, N_i number of inputs, N_o number of outputs). The discrete Fourier transformation $X(k) = F(x_n)$ of signal x_n is defined as

$$X(k) = F(x_n) = \frac{1}{\sqrt{N}} \sum_{n=0}^{N-1} x_n z_k^{-n} \tag{3}$$

with $z_k = e^{j2\pi k/N}$. Equivalent expressions can be obtained for the discrete Fourier transformation of the signals u_n and y_n as $U(k) = F(u_n)$ and $Y(k) = F(y_n)$, with discrete Fourier transform $F()$ defined by Eq. (3). The discrete Fourier transform of x_{n+1} is given by

$$F(x_{n+1}) = \frac{1}{\sqrt{N}} \sum_{n=0}^{N-1} x_{n+1} z_k^{-n} \tag{4}$$

$$= \frac{z_k}{\sqrt{N}} \sum_{n=0}^{N-1} x_n z_k^{-n} + \frac{z_k}{\sqrt{N}}(x_N - x_0) \tag{5}$$

$$= z_k X(k) + \frac{z_k}{\sqrt{N}}(x_N - x_0) \tag{6}$$

with $X(k)$ defined by Eq. (3). Taking the discrete Fourier transform of Eqs. (1) and (2) leads to

$$z_k X(k) = AX(k) + BU(k) + B_T \frac{z_k}{\sqrt{N}}, \tag{7}$$

$$Y(k) = CX(k) + DU(k) \tag{8}$$

with $B_T = x_0 - x_N$. This extension was introduced in Refs. [4,5] to describe state-space model in the frequency-domain under the same assumption as time domain methods, although in many identification methods the contribution of B_T is neglected. A sufficient condition to let B_T be zero is that the initial and final conditions are equal, which is the case for periodic and time-limited signals.

3. State-space model for FRF data

In case of arbitrary input signals the non-parametric H_1 estimator is often used in modal analysis [9,10] to estimate the FRFs.

$$H_1(\omega_k) = G_{YU}(\omega_k) G_{UU}(\omega_k)^{-1} \tag{9}$$

with $G_{YU}(\omega_k) = (1/N_b)\sum_{b=1}^{N_b} Y_b(k) U_b(k)^H$ and $G_{UU}(\omega_k) = (1/N_b)\sum_{b=1}^{N_b} U_b(k) U_b(k)^H$ and N_b the number of blocks in which the measured time data is divided. It can easily be proven that the H_1 estimator is consistent if only noise (uncorrelated with the input signals) on the measured responses y_n is present and the variance, i.e. uncertainty on the estimated FRFs reduces proportionally by $1/N_b$. Starting from FRFs has the advantage that the initial data set is reduced and the influence of the noise on the measurements is reduced by the averaging process. Although in practise one has to deal with a trade-off between the variance and bias on the FRF estimate. Given a data set with a limited amount of data, a choice must be made in the number of blocks. A large number of blocks will result in a large reduction of the noise levels, but introduces a bias error caused by the leakage, since a large number of blocks results in a small number of data samples within a block. The use of window techniques, e.g. a Hanning window reduces the effect of the leakage, but still significant bias errors are introduced, especially for low damped systems.

Our goal is to calculate an exact state-space model for the H_1 estimator that takes into account the initial and final conditions of each block. In this way both the data set and the uncertainty of the FRFs can be reduced without introducing errors caused by leakage. Substituting Eq. (7) in Eq. (8) leads to the following expression for block b:

$$Y_b(k) = \left(C(z_k I - A)^{-1} B + D\right) U_b(k) + C(z_k I - A)^{-1} B_{T,b} \frac{z_k}{\sqrt{N}}. \tag{10}$$

Right multiplication by $U_b^H(k)$ and summation over all N_b blocks results in

$$G_{YU}(\omega_k) = \left(C(z_k I - A)^{-1}B + D\right)G_{UU}(\omega_k) + C(z_k I - A)^{-1}[B_{T,1} \ \ldots \ B_{T,N_b}]\begin{bmatrix} \frac{z_k}{\sqrt{N}}U_1(k) \\ \vdots \\ \frac{z_k}{\sqrt{N}}U_{N_b}(k) \end{bmatrix}. \quad (11)$$

Multiplying both sides of Eq. (11) by $G_{UU}(\omega_k)^{-1}$ leads to an exact parametric model for the H_1 estimator.

$$H_1(\omega_k) = C(z_k I - A)^{-1}[B \ B_{T,1} \ \ldots \ B_{T,N_b}]\begin{bmatrix} I_{N_i} \\ T_1(k) \\ \vdots \\ T_{N_B}(k) \end{bmatrix} + D \quad (12)$$

with $T_b(k) = (1/\sqrt{N})z_k U_b(k)G_{UU}(\omega_k)^{-1}$ and I_{N_i} a unity matrix of dimension N_i. This extended FRF model clearly illustrates that the H_1 FRF estimate is the sum of a deterministic contribution $C(z_k I - A)^{-1} + D$ describing the structure under test and a stochastic contribution

$$C(z_k I - A)^{-1}[B_{T,1} \ \ldots \ B_{T,N_b}]\begin{bmatrix} T_1(k) \\ \vdots \\ T_{N_B}(k) \end{bmatrix}$$

introduced by the leakage (notice that $T_1(k)$ has the same random behavior as $U(k)$). Only if this stochastic contribution on the FRFs is taken into account by considering the initial conditions $B_{T,b}$, no bias errors are introduced. Eq. (12) can be rewritten as a state-space model

$$z_k X(k) = AX(k) + B'U'(k), \quad (13)$$

$$H_1(\omega_k) = CX(k) + D \quad (14)$$

with $B' = [B \ B_{T1} \ \ldots \ B_{TN_b}]$, $U'^{\mathrm{T}} = [I_{Ni} \ T_1^{\mathrm{T}} \ \ldots \ T_{N_b}^{\mathrm{T}}]$ and the state vector $X(k) \in \mathbf{R}^{N_i \times N_s}$. It is important to notice that this extended state-space model fits the FRFs calculated by the H_1 method exactly if a rectangular window is used (which is equal to not using a window). Furthermore, each extra block i used by the H_1 estimation introduces N_s extra parameters B_{Ti} in the model, while the equivalent common denominator approach in Refs. [3,2] introduces $N_o N_s$ extra parameters in the model.

4. Subspace identification

In Refs. [7,6] frequency-domain subspace algorithms have been developed for discrete- and continuous-time models. These methods have been successfully applied to real-life applications such as modal analysis, flight flutter testing and the modelling of synchronous machines. This

paragraph gives a short introduction and summary of a frequency-domain subspace algorithm to identify the state-space models from FRF data with their extension to take into account the initial and final conditions. The algorithm will be focussed on the state-space formulation (13) and (14). A more profound study about deterministic, stochastic, combined deterministic-stochastic frequency domain subspace identification and several practical applications can be found in Ref. [11].

Recursive use of Eqs. (13) and (14) gives

$$z_k^p H_1(\omega_k) = z_k^{p-1}(Cz_k X(k) + Dz_k) \tag{15}$$

$$= z_k^{p-1}(CAX(k) + CB'U'(k) + Dz_k) \tag{16}$$

$$\vdots$$

$$= CA^p X(k) + (CA^{p-1}B' + CA^{p-2}B'z_k + \cdots + CB'z_k^{p-1} + D'z_k^p)U'(k) \tag{17}$$

with $D' = [D\ 0]$ and D' a $N_s \times N_i + N_b$ matrix. Writing Eq. (17) for $p = 0, 1, \ldots, r-1$ on top of each other gives

$$\begin{bmatrix} H_1(\omega_k) \\ z_k H_1(\omega_k) \\ \vdots \\ z_k^{r-1} H_1(\omega_k) \end{bmatrix} = O_r X + \Gamma \begin{bmatrix} U'(\omega_k) \\ z_k U'(\omega_k) \\ \vdots \\ z_k^{r-1} U'(\omega_k) \end{bmatrix} \tag{18}$$

with O_r the extended observability matrix

$$O_r = \begin{bmatrix} C \\ CA \\ \vdots \\ CA^{r-1} \end{bmatrix} \tag{19}$$

and Γ a lower triangular block Toeplitz matrix.

$$\Gamma = \begin{bmatrix} D' & 0 & \ldots & 0 \\ CB' & D' & \ldots & 0 \\ \vdots & \vdots & \vdots & \vdots \\ CA^{r-2}B' & CA^{r-3}B' & \ldots & D' \end{bmatrix}. \tag{20}$$

Collecting Eqs. (18) for $k = 1, 2, \ldots, M$ with M the number of frequency lines in the chosen frequency band results in

$$\mathbf{H} = O_r \mathbf{X} + \Gamma \mathbf{U} \tag{21}$$

with $\mathbf{H}$ a complex $N_o N_r \times N_i M$ block Vandermonde matrix and $\mathbf{U}'$ a complex $(N_i + N_b)N_r \times N_i M$ block Vandermonde matrix defined by

$$\mathbf{H} = \begin{bmatrix} H_1(\omega_1) & H_1(\omega_2) & \dots & H_1(\omega_M) \\ z_1 H_1(\omega_1) & z_2 H_1(\omega_2) & \dots & z_M H_1(\omega_M) \\ \vdots & \vdots & \vdots & \vdots \\ z_1^{r-1} H_1(\omega_1) & z_2^{r-1} H_1(\omega_2) & \dots & z_M^{r-1} H_1(\omega_M) \end{bmatrix},$$

$$\mathbf{U} = \begin{bmatrix} U'(\omega_1) & U'(\omega_2) & \dots & U'(\omega_M) \\ z_1 U'(\omega_1) & z_2 U'(\omega_2) & \dots & z_M U'(\omega_M) \\ \vdots & \vdots & \vdots & \vdots \\ z_1^{r-1} U'(\omega_1) & z_2^{r-1} U'(\omega_2) & \dots & z_M^{r-1} U'(\omega_M) \end{bmatrix}$$

and $\mathbf{X}$ a complex N_s by $(N_i + N_b)M$ matrix defined by

$$\mathbf{X} = \begin{bmatrix} X(1) & X(2) & \dots & X(M) \end{bmatrix}.$$

Eq. (21) is converted in a set of real equations

$$\mathbf{H}^{\mathrm{re}} = O_r r \mathbf{X}^{\mathrm{re}} + \Gamma \mathbf{U}^{\mathrm{re}}, \tag{22}$$

where $()^{\mathrm{re}}$ locates the real and imaginary parts beside each other, for example

$$\mathbf{H}^{\mathrm{re}} = [\mathrm{Re}(\mathbf{H})\ \mathrm{Im}(\mathbf{H})]. \tag{23}$$

Eq. (23) with r larger than the model order N_s is the basic equation in frequency-domain subspace identification. Frequency-domain subspace identification algorithms are basically a four-step procedure. First, form the data matrices $\mathbf{H}^{\mathrm{re}}$ and $\mathbf{U}^{\mathrm{re}}$. Next, by using a QR-factorization, followed by an singular value decomposition the estimation of the extended observability matrix O_r takes place in an numerical efficient way [12].

$$\begin{bmatrix} \mathbf{U}^{\mathrm{re}} \\ \mathbf{H}^{\mathrm{re}} \end{bmatrix} = \begin{bmatrix} R_{11}^{\mathrm{T}} & 0 \\ R_{12}^{\mathrm{T}} & R_{22}^{\mathrm{T}} \end{bmatrix} \begin{bmatrix} Q_1^{\mathrm{T}} \\ Q_2^{\mathrm{T}} \end{bmatrix}, \tag{24}$$

$$R_{22}^{\mathrm{T}} = U \Sigma V^{\mathrm{T}}. \tag{25}$$

An estimate of $\hat{O}_r$ for model order N_s is given by

$$\hat{O}_r = U_{[:,1:N_s]}. \tag{26}$$

In a third step an estimate of A and C from $\hat{O}_r$ in a least-squares sense is given by

$$\hat{A} = \hat{O}^{+}_{[1:N_o(r-1),:]}\hat{O}_{[N_o+1:N_o r,:]} \text{ and } \hat{C} = \hat{O}_{[1:N_o,:]}. \tag{27}$$

In the fourth and last step the system matrixes B' and D given the estimates $\hat{A}$ and $\hat{C}$ are estimated in a least-squares sense from

$$H_1(\omega_k) = \hat{C}(Iz_k - \hat{A})^{-1}B'U'(k) + D. \tag{28}$$

5. Remarks

- From the A, B, C and D matrices the modal parameters as natural frequencies, damping ratios, mode shapes and participation factors can easily be recovered by a eigenvalue decomposition [13].
- Since a transient is simply the output of a system caused by initial conditions of the states different from zero, the model proposed by Eqs. (7) and (8) has exactly the same form as the model valid for periodic excitations corrupted with transients. Notice that the model matrices A and C can be estimated from transient signals only, if the input signals U are zero. Thus from transient responses only both the natural frequencies as mode shapes can be recovered. The B and D system matrices disappear in that case from the model in Eqs. (7) and (8).
- The exponential decay (stable system) of the transients in the outputs depends on the damping of the system. Therefore, lightly damped systems are more sensitive to errors due to leakage and transients than highly damped systems. So, in case of lightly damped systems, it is advised to use the extended state space formulation to avoid large errors on the damping ratios of the system.
- Notice that the extended formulation of the frequency-domain state-space model introduces N_b extra inputs in the first equation of the model respectively Eq. (7) in the case of input–output data and Eq. (14) in the case of FRF data. Furthermore, this extended model can be used to model only transient responses of a system in case no input signal is applied. Notice that from these transient responses both the A and C matrices can be obtained. In applications like model analysis these system matrices contain the natural frequencies, damping values and mode shapes.
- The covariance matrix of the disturbing noise can be used as a weighting in the algorithm to be consistent [7]. In Ref. [14] it is proven that this still holds if the true covariance matrix is replaced by the covariance matrix obtained from a small number of averaged blocks.
- In modal analysis, time-domain algorithms often start from Impulse Response Functions (IRF) from FRFs. These IRFs are often estimated, e.g. by a H_1 estimator (to reduce the noise) followed by an inverse discrete Fourier transform. As a result, such a time-domain approach suffers from the leakage in the FRFs and thus in the IRFs. The proposed identification procedure in this article allows to start the identification from FRF data without suffering from any errors introduced by leakage phenomena.

6. Simulation and real measurement examples

6.1. Noise-free simulations

The goal of this simulation is to illustrate that model (13) and (14) is exact without any approximation and that neglecting the influence of leakage can lead to large uncertainties on the estimated models.

A sixth-order MIMO discrete-time domain system is excited with Gaussian white noise. The A, B, C and D matrices used for the simulation are given in the appendix. Two different Monte Carlo tests (100 runs each) with different number of time samples $N = 4096$ and 1024 are performed. The respectively 4096 and 1024 simulated time samples of the output and input signal are divided in 4 equal data blocks of respectively 1024 and 256 time samples. No disturbing noise is added to the signals in order to focus the simulation study on the errors introduced by leakage. In each of the 100 runs of both Monte Carlo tests the simulated data is processed in two different ways:

- *Classic state-space model* (CSSM): The spectra of the 4 data blocks ($N_b = 4$) are calculated by using a Hanning window to reduce the effect of leakage. In a next step the FRFs are estimated by the H_1 non-parametric estimator (9). In the last step a state space model ($N_s = 10$) is fitted through the FRF data by using the frequency-domain subspace approach.
- *Extended state-space model* (ESSM): The spectra of the 4 data blocks are calculated by using a rectangular window. In a next step the FRFs are estimated by the H_1 non-parametric estimator. In the last step an extended state space model (13) and (14) ($N_s = 10$) is fitted through the FRF data by using the proposed frequency-domain subspace approach.

Assume the sample rate to be 1 Hz and thus the Nyquist frequency 0.5 Hz. The poles p_c in the continuous time domain are given by the logarithmic function $p_c = \log(p_z)$ of the discrete time-domain poles p_z. The model used for the simulation has three complex conjugate pairs of poles. The natural frequency and damping ratio are respectively defined by $f = \omega/(2pi)$ and $d = \sigma/\sqrt{\sigma^2 + \omega^2}100$ (in %) with $p_c = -\sigma + j\omega$. Tables 1 and 2 show respectively the results of the Monte Carlo simulations with 4096 and 1092 time samples. The relative error $\Delta\alpha$ of a parameter α is defined by std(α)/mean(α) with std the standard deviation over the 100 runs.

Using the classic state-space model Table 1 shows the that the relative error of the natural frequencies is lower than 1%, but the damping ratio suffers from larger errors (up to 28%),

Table 1
Monte Carlo simulation 1 (4096 samples)

f_{exact} (%)	d_{exact} (%)	Classic model (%)		Extended model (%)	
		Δ_f	Δ_d	Δ_f	Δ_d
0.13	0.49	0.2740	28.6313	0.0000	0.0005
0.25	0.89	0.0334	3.8505	0.0000	0.0010
0.33	1.16	0.0126	2.1087	0.0000	0.0066

Table 2
Monte Carlo simulation 1 (1024 samples)

f_{exact} (%)	d_{exact} (%)	Classic model (%)		Extended model (%)	
		Δ_f	Δ_d	Δ_f	Δ_d
0.13	0.49	1.3398	68.9488	0.0000	0.0070
0.25	0.89	0.4868	34.8320	0.0001	0.0081
0.33	1.16	0.1500	14.7810	0.0001	0.0179

although the processed time series are relatively long. In particular the low-frequency poles suffer from large errors, since they are more sensitive for errors due to leakage phenomena. When the same simulated time series are processed by modelling an extended state-space model, which takes into account the initial and final conditions the errors decrease drastically below 0.01%, which is the level of the computational errors. Table 2 shows that the errors increase a lot by decreasing the number of time samples from 4096 to 1024 when a classic state-space model is used, while the proposed extended model still results in very accurate estimates. The FRFs contain only 128 spectral lines in this second Monte Carlo simulation. Fig. 1 illustrates the H_1 estimate from the four blocks of 256 samples with a Hanning window, the synthesized FRF of the classic state-space model and the exact FRF. Although the H_1 estimate of the FRF looks acceptable compared to the exact FRF, the synthesized FRF does not fit the exact FRF due to the model errors caused by the leakage. The H_1 estimate with a rectangular window in Fig. 2 looks worse compared to the FRF obtained by using a Hanning window, although the synthesized FRF from the extended state-space model perfectly fits the exact FRF since the initial and final conditions of each block are properly taken into account.

6.2. Noise-corrupted simulations

In a second set of simulations the response measurements $y(n)$ are corrupted by colored noise $y_r(n)$. For each of the 100 Monte Carlo runs the '4096' time samples are processed by the CSSM and ESSM approach for different numbers of blocks used in the H_1 FRF estimation. The mean square error (MSE) of the damping ratios from the 100 Monte Carlo runs is calculated as the

$$\mathrm{MSE} = \frac{1}{100}\sum_{i=1}(\hat{d}_i - d_e)^2 \tag{29}$$

with $\hat{d}_i$ the estimated damping ratio and d_e the exact damping ratio. The mean square error is equal to the sum of the variance and square of the bias.

Fig. 3 clearly shows the trade-off between variance and bias for the CSSM approach. The classical H_1 approach reduces the noise levels on the FRFs by averaging, but the bias due to leakage increases by decreasing the blocks length. Based on this trade-off the user has to the define the number of blocks. Notice that the optimal number of blocks not known a priori and depends on the total measurement time and the modal density in the measurements. The ESSM approach clearly improves the quality of the estimates from this noise data, since the noise is reduced

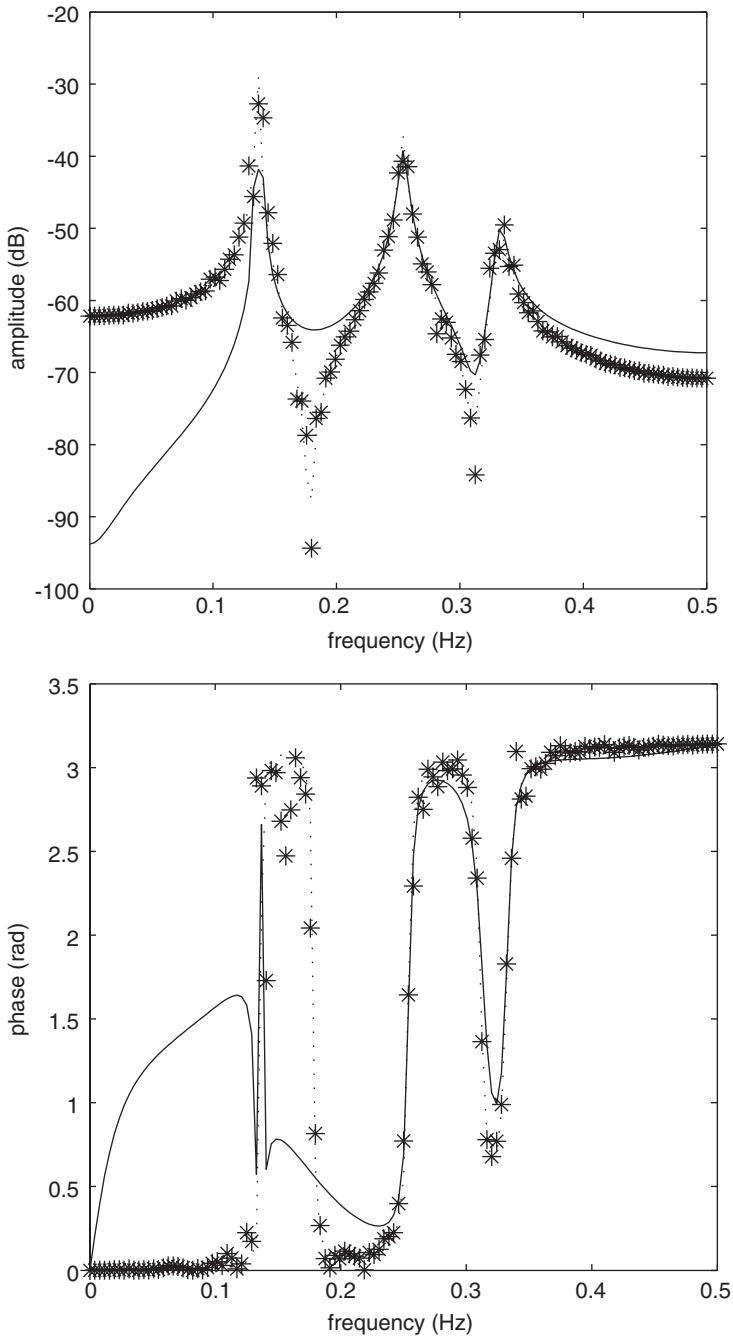

Fig. 1. Comparison between the exact FRF (dotted line), H_1 FRF estimate by using a Hanning window (*) and the synthesized FRF for the CSSM model (full line).

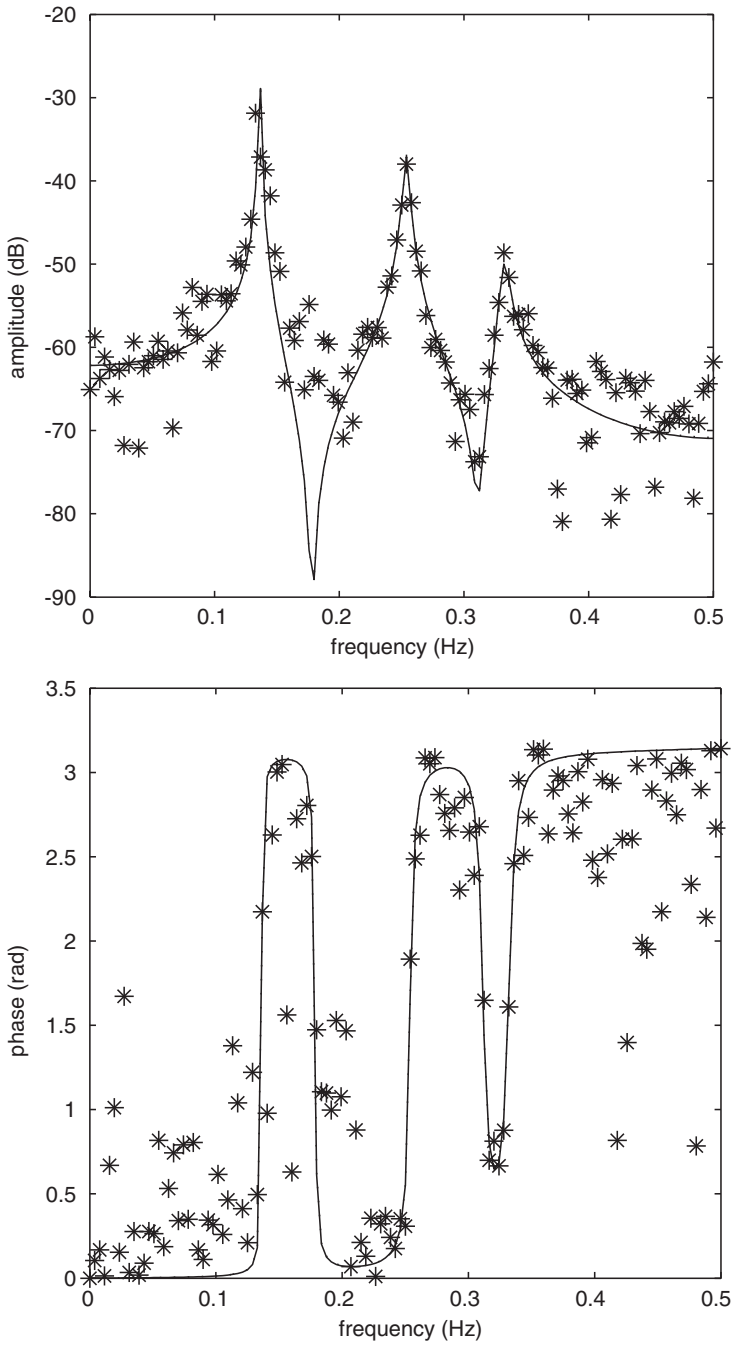

Fig. 2. Comparison between the exact FRF (dotted line), the H_1 FRF estimate by using a rectangular window (*) and the synthesized FRF for the ESSM model (full line).

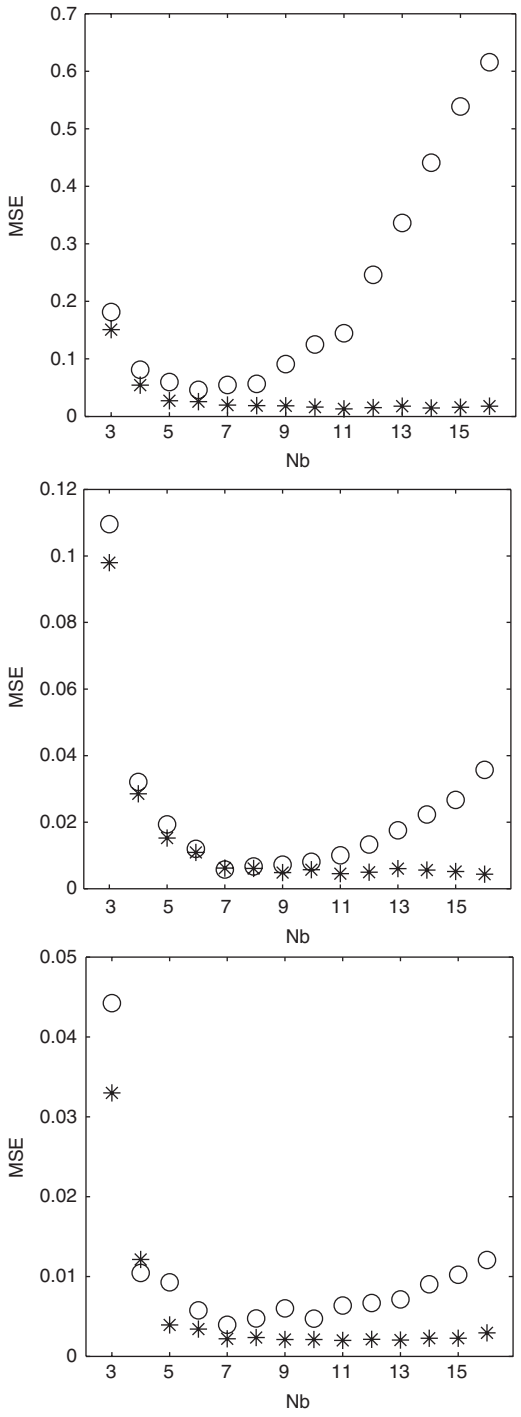

Fig. 3. Mean square error (MSE) of the damping ratio estimates of the CSSM approach (○) and ESSM approach (✻) for different number of blocks.

without introducing bias errors due to leakage. In this way the MSE reduces and becomes much less dependent of the number of blocks.

6.3. Real measurement example

Fig. 4 shows the measurement setup to perform a modal analysis of an engine subframe. Two shakers excite the structure with a random force. A sample rate of 2048 Hz is used and 256 K

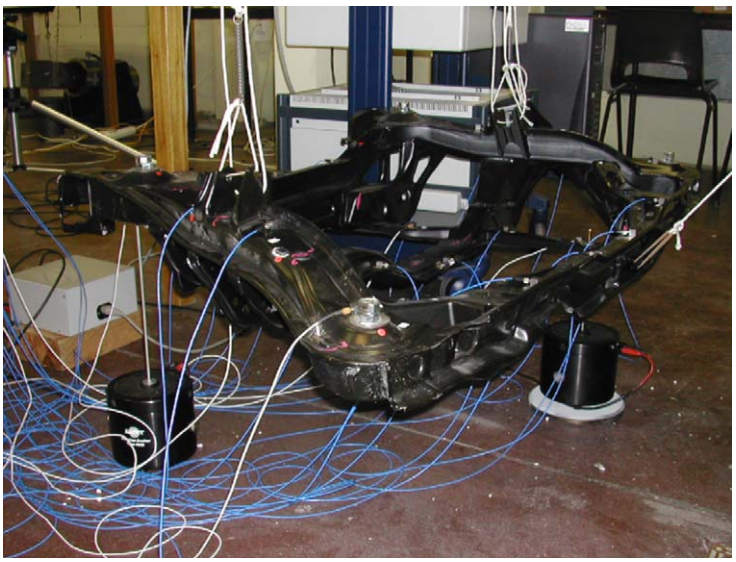

Fig. 4. MIMO measurement setup of an engine subframe of a car.

Table 3
Natural frequencies and damping ratios of the subframe

f_{ref}	f_{ESSM}	f_{CSSM}	d_{ref}	d_{ESSM}	d_{CSSM}
129.5	129.5	130.3	0.122	0.116	0.202
147.8	147.9	148.1	0.081	0.081	−0.002
175.9	176.3	176.0	1.138	1.118	0.208
205.6	205.6	204.8	0.106	0.112	0.110
241.0	241.0	241.4	0.115	0.110	0.160
252.9	252.9	253.0	0.095	0.091	0.102
286.3	286.3	286.7	0.221	0.224	0.291
291.2	291.5	–	1.006	0.801	–
329.3	329.3	329.6	0.164	0.164	0.214
331.3	331.3	331.3	0.130	0.134	0.277
356.1	356.1	355.8	0.099	0.099	0.212
359.7	359.7	359.5	0.101	0.101	0.306
379.7	379.7	379.8	0.142	0.143	0.061
402.6	402.6	402.3	0.098	0.097	0.148

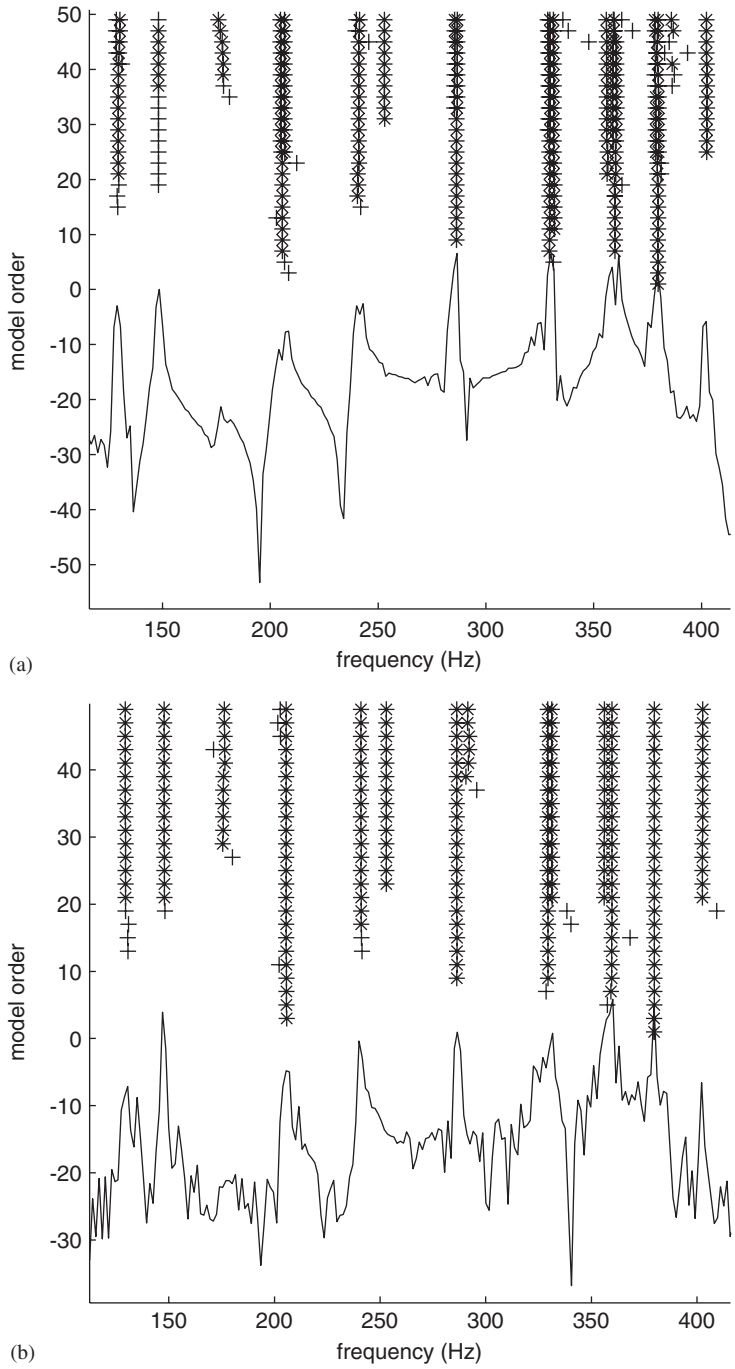

Fig. 5. Stabilization diagrams: (a) CSSM approach, (b) ESSM approach. +, Unstable pole; *, stable pole.

(1 K = 1024) samples are measured. First all 256K time samples of both acceleration and force measurements are divided in 8 long blocks resulting in a frequency-domain resolution of 0.0156 Hz. Since the length of these blocks is very long (64K), the spectra and the calculated FRFs are considered as leakage free and as a reference. These leakage-free FRFs lead to the reference modal parameters. Next only the first 8K data samples are used and divided in 4 equal blocks of each 2K samples resulting in a frequency resolution of 1 Hz. First the FRFs are calculated by the H_1 method with a Hanning window. From these FRFs a classic state-space model is estimated with a frequency-domain subspace method. Secondly the same 4 blocks of data are used to obtain the FRFs with a rectangular window. These FRFs are processed to estimate an extended state-space model. Table 3 shows the good agreement between the natural frequencies and damping ratios obtained from the reference FRFs and the estimates derived from the short data sequences with the ESSM approach. The use of a Hanning window and a classic state-space identification clearly results in poor estimates, especially the damping estimates.

A typical tool in commercial modal analysis software to distinguish mathematical poles from physical poles is a stabilization diagram. This diagram shows the estimated poles for different model orders. Fig. 5 shows the stabilization diagram for both the CSSM approach and the ESSM approach. Although the ESSM approach does not use a Hanning window and as a result the FRF looks much noisier, all the poles clearly appear in the stabilization diagram. The CSSM approach suffers from estimating double poles, where only one physical pole is present e.g. around 129, 205, 286 and 380 Hz. This is typically caused by leakage phenomena and makes the stabilization diagram confusing for the end-user. Finally, Fig. 6 compares the synthesized FRFs of both

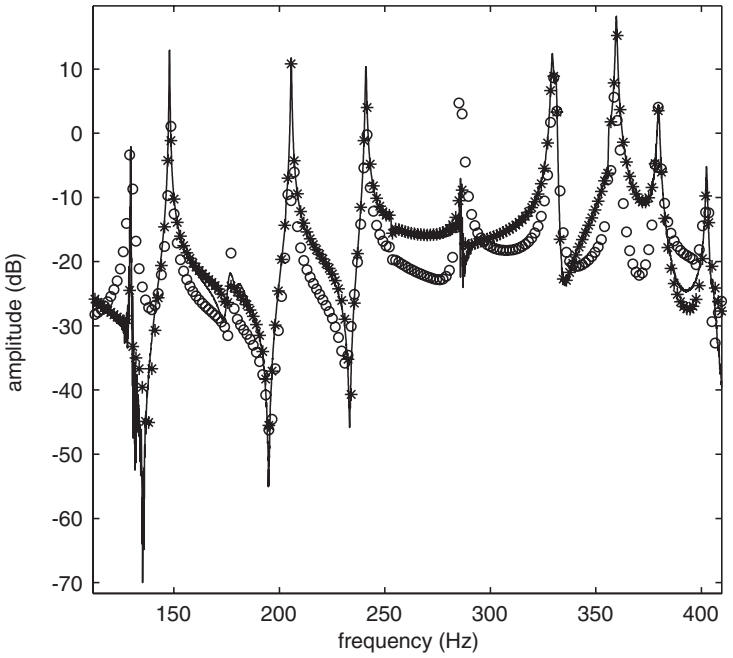

Fig. 6. Comparison between the reference FRF (full line), the synthesized FRF from the CSSM model (○) and the synthesized FRF from the ESSM model (∗).

approaches with the reference FRF from the leakage free measurement. One concludes that although the extended model approach started from only 8K data samples, averaged in 4 blocks of 2K samples, still a very good agreement is found between the model and the reference FRFs, while a classic approach clearly fails due to errors introduced by leakage.

7. Conclusions

This paper shows how frequency-domain state-space models for FRF data can handle arbitrary input signals and transients without introducing systematic errors. Adding the initial and final conditions of the states for every data block in the state-space model allows to identify discrete-time models in the frequency domain without any approximation. This allows to reduce the initial data set and the uncertainty on the final parameters without introducing a bias caused by leakage. A frequency-domain subspace algorithm was applied to identify the state-space matrices together with initial/final conditions of each block. The presented method improves the modal parameter estimates and especially the damping ratio estimates. Furthermore, the final estimates of the parameters are much less dependant from the number of blocks averaged for the estimation of the FRFs. The proposed method is evaluated by both a simulation and a real-life measurement example.

Acknowledgements

The financial support of the Fund for Scientific Research (FWO Vlaanderen), the Concerted Research Action "OPTIMech" of the Flemish Community; the Research Council (OZR) of the Vrije Universiteit Brussel (VUB); Federal Government IUAP V/22; the Concerted Research Action "ILiNOS" of the Flemish Community are gratefully acknowledged. The first author holds a Research Assistant Grant of the Fund for Scientific Research-Flanders (Belgium) (F.W.O.-Vlaanderen) at the mechanical engineering department of the Vrije Universiteit Brussel.

Appendix

Simulation model:

$$A = \begin{bmatrix} 0.6541 & -0.8108 & -0.0009 & -0.0042 & 0.0003 & 0.0018 \\ 0.6977 & 0.6512 & 0.0004 & 0.0031 & -0.0001 & -0.0013 \\ -0.0007 & 0.0050 & -0.0211 & -1.0106 & 0.0131 & -0.0436 \\ 0.0001 & -0.0001 & 0.9599 & -0.0270 & -0.0079 & 0.0165 \\ -0.0003 & 0.0019 & -0.0118 & -0.0442 & -0.4961 & 0.9079 \\ 0.0002 & -0.0016 & 0.0027 & 0.0176 & -0.7944 & -0.4636 \end{bmatrix},$$

$$B = \begin{bmatrix} -0.0018 & -0.0025 \\ 0.0010 & 0.0014 \\ -0.0014 & 0.0000 \\ 0.0004 & -0.0000 \\ 0.0007 & -0.0010 \\ -0.0001 & 0.0002 \end{bmatrix},$$

$$C = \begin{bmatrix} -0.1735 & -0.0301 & -0.2569 & 0.0922 & 0.1920 & 0.0696 \\ -0.2453 & -0.0435 & -0.0054 & -0.0114 & -0.2753 & -0.0786 \\ -0.1736 & -0.0318 & 0.2650 & -0.0744 & 0.1976 & 0.0408 \end{bmatrix},$$

$$D = \begin{bmatrix} 0.1327 & -0.0085 \\ -0.0085 & 0.1322 \\ -0.0006 & -0.0085 \end{bmatrix} 1.0e-003.$$

References

[1] R. Pintelon, J. Schoukens, G. Vandersteen, Frequency domain system identification using arbitrary signals, *IEEE Transactions on Automatic Control* 43 (12) (1997) 1717–1720.

[2] B. Cauberghe, P. Guillaume, P. Verboven, Steve Vanlanduit, E. Parloo, Frequency response function based parameter identification from short data sequences, *Mechanical Systems and Signal Processing (MSSP)* 18 (5) (2004) 1097–1116.

[3] B. Cauberghe, P. Guillaume, Frequency response functions based parameter identification from short data sequences, in: *Proceedings of the Eighth International Conference on Recent Advances in Structural Dynamics*, Southampton (UK), July 2003.

[4] T. McKelvey, Frequency domain identification, in: *Preprints of the 12th IFAC Symposium on System Identification*, Santa Barbara, CA, USA, June 2000.

[5] T. McKelvey, Frequency domain identification methods, *Circuits Systems Signal Processing* 21 (1) (2002) 39–55.

[6] P. Van Overschee, B. De Moor, Continuous time–frequency domain subspace system identification, *Signal Processing* 52 (2) (1996) 179–194.

[7] T. McKelvey, H. Akcay, M. Ljung, Subspace-based multivariable system identification from frequency response data, *IEEE Transactions on Automatic Control* 41 (7) (1996) 960–978.

[8] P. Van Overschee, B. De Moor, *Subspace Identification For Linear Systems*, Kluwer Academic Publishers, Dordrecht, 1996.

[9] N.M. Maia, J.M. Silva, *Theoretical and Experimental Modal Analysis*, Wiley, New York, 1997.

[10] W. Heylen, S. Lammens, P. Sas, *Modal Analysis Theory and Testing*, K.U. Leuven, 1998.

[11] B. Cauberghe, *Application of Frequency–domain System Identification for Experimental and Operational Modal Analysis*, PhD Thesis, Department of Mechanical Engineering, Vrije Universiteit Brussel, Belgium, downloadable www.avrg.vub.ac.be, 2004.

[12] M. Verhaegen, Identification of the deterministic part of mimo state space models given in innnovations from input–output data, *Automatica* 30 (1) (1994) 61–74.

[13] Jer-Nan Juang, *Applied System Identification*, Prentice-Hall, Englewood Cliffs, NJ, 1994.

[14] R. Pintelon, Frequency-domain subspace system identification using non-parametric noise models, *Automatica* 38 (2002) 1295–1311.